A MAGNETIC SURVEY OF THE SOUTHERN SOCORRO MOUNTAINS NEW MEXICO

by

R. Ramananantoandro

Submitted in partial fulfillement of the
requirements for the degree of
MASTER OF SCIENCE IN GEOPHYSICS
New Mexico Institute of Mining and Technology
August 1965

CONTENTS

LIST OF FIGURES

LIST OF TABLES

LIST OF PLATES

Plate

ACKNOWLEDGMENT

The work presented in this paper was performed under the direction of Dr. Allan R. Sanford of the New Mexico Institute of Mining and Technology. The author takes the opportunity to express his appreciation to Dr. A. R. Sanford for his counseling during the period of investigation and his great assistance in the preparation of this report. The author is also indebted to Mr. R. W. Foster and Mr. M. E. Willard of the New Mexico Bureau of Mines and Mineral Resources for their helpful suggestions. The assistance of R. Srinivas Ravula, Lawrence Schuster, Gary Sower and Van Taylor in the field or in the analysis of the data is gratefully acknowledged.

ABSTRACT

A magnetic survey of the southern part of the Socorro Mountains revealed simple and broad anomalies due to deep-seated structures. As gravity data of the same area was available, a combined analysis of the gravity and magnetic anomalies was attempted to determine the susceptibility of the rocks comprising these structures. The analysis failed because the magnetic map computed from the gravity data did not match the observed magnetic data.

A quantitative interpretation of two of the broad anomalies in terms of geological structure was made. Intrusions or buried flows of basic rocks were assumed to be responsible for the high anomalies. A tabular body 1470 m wide at a depth of 735 m is proposed for one anomaly, and a stock with a diameter of 2.1 km at a depth of 2.3 km is proposed for the other.

A MAGNETIC SURVEY OF THE SOUTHERN SOCORRO MOUNTAINS NEW MEXICO

INTRODUCTION

The Socorro mountains are a part of a series of fault block mountains beginning with the Ladron Mountains to the north and dying out to the south in the Chupadera Mountains. The uplifted Socorro block plunges gently to the south. Although composed of Precambrian, Pennsylvanian, Tertiary and Quaternary rocks, only Tertiary and Quaternary rocks are exposed in the area surveyed. The Tertiary units are mainly igneous rocks, ranging from acidic to basic. This makes the the magnetic method quite fit for a study of the geological structure, since the greater the susceptibility contrasts between the different units the larger the resultant anomalies.

The purpose of the work presented in this paper is to determine the structures that are responsible for the high magnetic anomalies measured with a vertical magnetometer. This interpretation is based on the surface geology, the measured magnetic susceptibilities of the representative rocks of the area, and the shape and magnitude of the magnetic anomalies.

The results presented here are approximate. Detailed structural analyses of the anomalies require long and laborious computations. Since no computer was available, simplifying assumptions as to the shape, direction of field, etc. were made in order to make some calculations possible.

GEOLOGY OF THE AREA

The area covered by the survey is the southern part of the Socorro Mountains and adjacent valley areas that lie between 34°00′ - 34°03′ north latitude and 106°53′ - 107°04′ west longitude. It covers about 40 square miles. The mountainous terrain covered by the survey is almost entirely composed of Tertiary igneous rocks overlying Pennsylvanian and Precambrian rocks, that are not exposed. The igneous rocks range from rhyolite to basalt and are in the form of intrusions (plug, dike) or flows. The valley portions of the survey are for the most part covered with Quaternary alluvium. A detailed geologic map of the area is not available, but a rough map giving a general idea of the geology is shown in Plate I.

Mr. Max Willard of the New Mexico Bureau of Mines and Mineral Resources is mapping the region south of US Highway 60 and has found the following stratigraphic sequence (personal communication) :

Playa deposits

Datil
- Rhyolite
- Andesite - Basalt
- Rhyolite
- Andesite

Pre-volcanic rocks

Assuming both areas to be similar, the Quaternary basalt flow that constitutes the upper portion of Black Mountain overlies the playa deposits, the thickness of which is unknown.

MAGNETIC SUSCEPTIBILTY MEASUREMENTS

Samples of representative rocks of the area were collected and the magnetic susceptibility of each measured with a magnetic susceptibility bridge (Model MS-3, Geophysical Specialities Company, Minnesota). Each sample was ground to 48 mesh, a size that gives the most consistent measurements (R. Foster, personal communication). Table I shows the results of the susceptibility measurements and the location of the outcrops where the samples were collected.

In general the susceptibilities measured were found lower than normal (Dobrin 1960). The bridge gave a value of 912. 10^{-6} cgs for a sample of basalt from the Black Mountain (sample No 10, Table 1). The same sample of basalt was ground beyond 200 mesh and the magnetite content separated from the powder with a magnetic separator. The volume of magnetite separated was 0.26% of the total volume of the sample. Assuming the magnetization in a rock due mainly to the magnetite and assigning a susceptibility of 0.3 cgs (Dobrin 1960) to the magnetite , the susceptibility of a basalt containing 0.26% of magnetite in volume is 780. 10^{-6}cgs. This value agrees well with the value given by the bridge. The low values measured by both methods could be explained by a surface or near surface alteration of the magnetite in the rocks to other minerals.

A thin section of the same sample of basalt was made and

it was found to contain about 8% of opaque minerals (R. Foster , personal communication). The opaque minerals could be hematite as well as magnetite . But assuming the hematite to be a product of alteration of the magnetite, the susceptibility of that basalt would be 24,000. 10^{-6} cgs, a value which is about ten times higher than the highest value measured for the basalt from the Black Mountain. This assumption will be justified later in the interpretation of Anomaly B.(page 33).

Rock type	Location	Susceptibility k.10-6 cgs	
1. andesite	106°58'.3 34°00'.3	107	
2. andesite	106°58'.3 34°00'.3	48	
3. andesite	106°59'.5 34°00'.1	48	
4. andesite	106°59'.3 34°00'.4	29	
5. andesite	106°58'.7 33°59'.1	310	Average:
6. andesite	106°59'.6 34°00'.6	48	115. 10^{-6}cgs
7. andesite*		155	
8. andesite*		145	
9. andesite*		145	
10. basalt	106°59'.3 34°00'.8	912	
11. basalt	106°59'.6 34°00'.7	3056	Average:
12. basalt	106°59'.3 34°00'.8	727	1504. 10^{-6}cgs
13. basalt	106°59'.6 34°00'.7	1426	
14. diabase*		1400	
15. rhyolite*		87	
16. rhyolitic breccia	106°56'.3 34°02'.5	359	
17. alluvium	106°54'.5 34°02'.0	456	

* No map of the area is available to give the exact location.

Table 1 Susceptibilities of samples of rocks

SURVEY PROCEDURE

Field Procedure

The magnetic measurements were taken with a Schmidt-type vertical magnetometer (Scout Model, Ruska Instrument Corporation, Texas). The characteristics of the instrument are:

1) Sensitivity : 25 γ per scale division

2) Temperature correction : 0.2 γ per unit (1 $^{\circ}$ C) increase of temperature.

Because a prospecting magnetometer of the type used measures relative values of the magnetic field, a base station was chosen and the reading at that point selected as a reference for the subsequent readings. In this survey, the base station was established in the Rio Grande Valley at a point easily accessible from US Highway 60 (see Plate II). Secondary base stations were used whenever the area surveyed was too far from the primary base station. All readings were taken at points that were easy to locate on the map and in the field, e.g. prominent topographic features, intersections of trails, elevation bench marks and section corner markers. The base map used were the USGS Socorro Quadrangle and Magdalena Quadrangle topographic sheets with scales of 1:62500 (Plate II).

Corrections and Presentation of the Data

The magnetometer readings converted into gammas were corrected for:

1) The diurnal variation of the earth's magnetic field. Readings at a base station were repeated approximately every two hours. The variation in magnetic reading over that time interval was assumed to be linear.

2) The decrease of 0.2 γ of the magnetic reading per increase of 1°C of the temperature. Considering the magnitude of the magnetic anomalies detected, this correction could be neglected.

3) The latitude and longitude variation. The magnetic charts of the United States for 1945 published by the USCGS, were used to remove the effect of the regional variation in the magnetic field from the magnetic map.

Table 2 shows a sample correction of a magnetometer reading, and Table 3 the list of all the stations with their corresponding corrected magnetic anomalies. These values were plotted on a map and contoured at 50 intervals (see Plate III)

With a complicated volcanic area as Socorro Mountains, one expects a complicated magnetic map. However the anomalies obtained are fairly simple and large. The simplicity of the magnetic map can be explained by the fact that one geologic unit (basalt or diabase) has a very high susceptibility

compared to the susceptibility of the rest of the rocks. Thus qualitatively the high anomalies can be interpreted as due to intrusions or buried flows of rocks of basaltic compositon.

station	time	(t°-20°)C	magneto-meter mean readings	readings in γ	correction in γ temp.	diur.	lat.long.	corrected readings in γ	-base sta.	-base sta. + 500
base	09:40	10	35.8	895.0	2.0	0	0	897	0	500
1	10:15	13	33.9	847.5	2.6	9.7	7	853	44	456
2	10:40	13	33.55	838.75	2.6	13.7	5	850	47	453
3	11:05	14	33.05	826.25	2.8	13.7	2	841	56	444
4	11:30	15	34.05	851.25	3.0	13.7	1	869	28	472
5	11:55	15	31.3	782.5	3.0	13.7	5	804	93	407
base	12:20	16	35.2	880.0	3.2	13.8	0	897	0	500

Table 2. Correction table of magnetometer readings.

Table 3 Station Numbers and Anomalies

Sta.	Ano.	Sta.	Ano.	Sta.	Ano.	Sta.	Ano.
B	500	24	370	40	495	68	405
1	456	25	411	41	690	69	425
2	453	B'	393	43	437	70	401
3	444	26	996	44	516	71	462
4	472	2*	819	45	547	72	353
5	407	3*	1058	46	356	74	385
6	524	4*	945	47	375	75	358
7	478	5*	1064	48	504	76	357
8	426	6*	871	49	562	77	622
9	455	7*	902	50	526	78	524
10	578	8*	1389	51	748	79	356
11	662	9*	571	53	510	80	471
12	556	10*	724	54	386	81	521
13	631	11*	857	55	334	82	510
14	740	27	663	56	446	83	442
15	812	28	302	57	477	84	518
16	587	29	498	58	485	85	418
17	588	30	446	59	483	86	360
18	596	31	1054	60	612	87	400
19	311	32	362	63	512	88	665
20	350	33	447	64	360	89	567
21	386	34	412	65	193	90	483
22	342	35	372	66	290		
23	501	37	249	67	297		

* Stephens readings (1962)

METHOD OF ANALYSIS

Introduction

In a quantitative magnetic interpretation, as in all potential field problems, there is no unique solution. When geologic or other control is available, one or more parameters of the problem may be determined, thus reducing the choice of solutions.

Two general approaches are used in a quantitative interpretation of field measurements in terms of geologic structures:

1) Theoretical profiles computed for simple geometrical structures are available. If any assumptions as to the shape of the anomaly-producing structure can be made, a profile of the observed anomaly is compared to a corresponding set of theoretical profiles. From the theoretical curve which best fits the observed curve, one can derive the shape, the depth, the dimensions, the orientation and the magnetic susceptibility of the buried structure.

2) On the basis of the shape of the anomaly and the geology of the surveyed area, a simple geometrical structure of fixed susceptibility is assumed. The resultant anomaly over this structure is computed

and compared to the observed curve. The dimensions, depth, susceptibility are varied until the calculated profile matches the observed profile.

In addition to these methods, a third approach was attempted in this work. The anomaly produced by a certain body in a field of force is a function of the anomalous property of the body and a potential factor which is a function of the shape and position of the body. If the same structure produces anomalies in two different fields of force, e.g. gravity and magnetic, the potential factor can be eliminated to give a relation between the two anomalous properties, and this relation will be independent of the shape and position of the body. In favourable cases, this method can determine the magnetic susceptibility of the rock, without knowing the dimensions and position of the structure.

As gravity data (after work by A. R. Sanford) was available in the same region as the magnetic survey (see Plate IV), an attempt was made to determine the magnetic susceptibility of the buried structures with this technique.

Combined Analysis of Gravity and Magnetic Anomalies

Theory

The theory of combined analysis of gravity and magnetic anomaly has been described by Garland (1951) and Lundbak (1956).

The expression of the potential at a point P due to a

magnetic dipole of magnetic moment M is

$$U_P = M \frac{\partial}{\partial m} \left(\frac{1}{r} \right), \qquad (1)$$

where m is the direction of magnetization and r the distance from the point of observation to the middle of the dipole. If an element of volume dv of magnetization I is considered, M can be expressed as

$$M = I\,dv. \qquad (2)$$

Substituting equation (2) into equation (1) gives

$$U_P = I\,dv \frac{\partial}{\partial m} \left(\frac{1}{r} \right). \qquad (3)$$

Now let ρ be the density of the same element of volume dv. The gravitational potential of dv at the point P is

$$V_P = G\rho \frac{dv}{r}, \qquad (4)$$

where G is the gravitational constant.

Rearranging equation (4) gives

$$\frac{1}{r} = \frac{V_P}{G\rho\,dv}, \qquad (5)$$

which when substituted into equation (3) gives

$$U_P = I\,dv \frac{\partial}{\partial m} \left(\frac{V_P}{G\rho\,dv} \right). \qquad (6)$$

Assuming I and ρ constant, the magnetic potential for the whole body is

$$U_P = \frac{I}{G\rho} \frac{\partial}{\partial m} \left(V_P \right). \qquad (7)$$

In a system of axes where the z-axis is positive downward, the derivative of equation (7) with respect to z is

$$Z = \frac{\partial U_P}{\partial z} = \frac{I}{G\rho} \frac{\partial^2}{\partial m \partial z} \left(V_P \right), \qquad (8)$$

the vertical component of the magnetic field.

Equation (8) can be written in the form

$$Z = \frac{I}{G\rho} g_m, \qquad (9)$$

where g_m is the gradient of the gravity at the point P in the direction of the magnetization.

Considering the magnetization in a structure induced by the earth's magnetic field, the direction of the magnetization is defined by the the declination d and the inclination i of the earth's magnetic field. Therefore g_m can be written

$$g_m = g_z \sin i + g_d \cos i, \qquad (10)$$

where g_z is the vertical gradient of the gravity and g_d is the horizontal gradient in the direction of the declination d. Finally the vertical component of the magnetic field is

$$Z = \frac{I}{G\rho} \left(g_z \sin i + g_d \cos i \right). \qquad (11)$$

The quantity between the brackets can be calculated since i is known and g_z and g_d can be derived from a gravity map. The quantity thus computed has to be multiplied by a constant factor, $\frac{I}{G\rho}$, in order to get the observed anomalies. Therefore if the general configuration of the computed magnetic

map agrees with the observed magnetic map, the constant factor $\frac{I}{G\rho}$ can be deduced. Since

$$I = kT \qquad (12)$$

where T is the strength of the earth's magnetic field, and k the magnetic susceptibility of the body, it is possible to determine the value of k knowing the value of the constant $\frac{I}{G\rho}$. The magnetic susceptibility determined by this method is more reliable than the susceptibility measured with a bridge since it represents an average value for the whole body. The bridge measures the susceptibility of a very small sample of the body, and the magnetite in the sample selected may be altered by weathering or may be of an amount which is not representative of the rock as a whole.

Application

Determination of the Inclination i. Since the magnetization of the body is considered induced by the earth's magnetic field, its direction is defined by the direction of the earth's magnetic field, i.e. inclination 62° and declination N 13°E.

Determination of the Horizontal Gradient g_d. The horizontal gradient of the gravity in the direction of the declination (N 13°E) is measured on the gravity map by taking

$$g_d = \frac{\Delta g}{\Delta \ell} \qquad (13)$$

The distance was chosen so that g varies uniformally

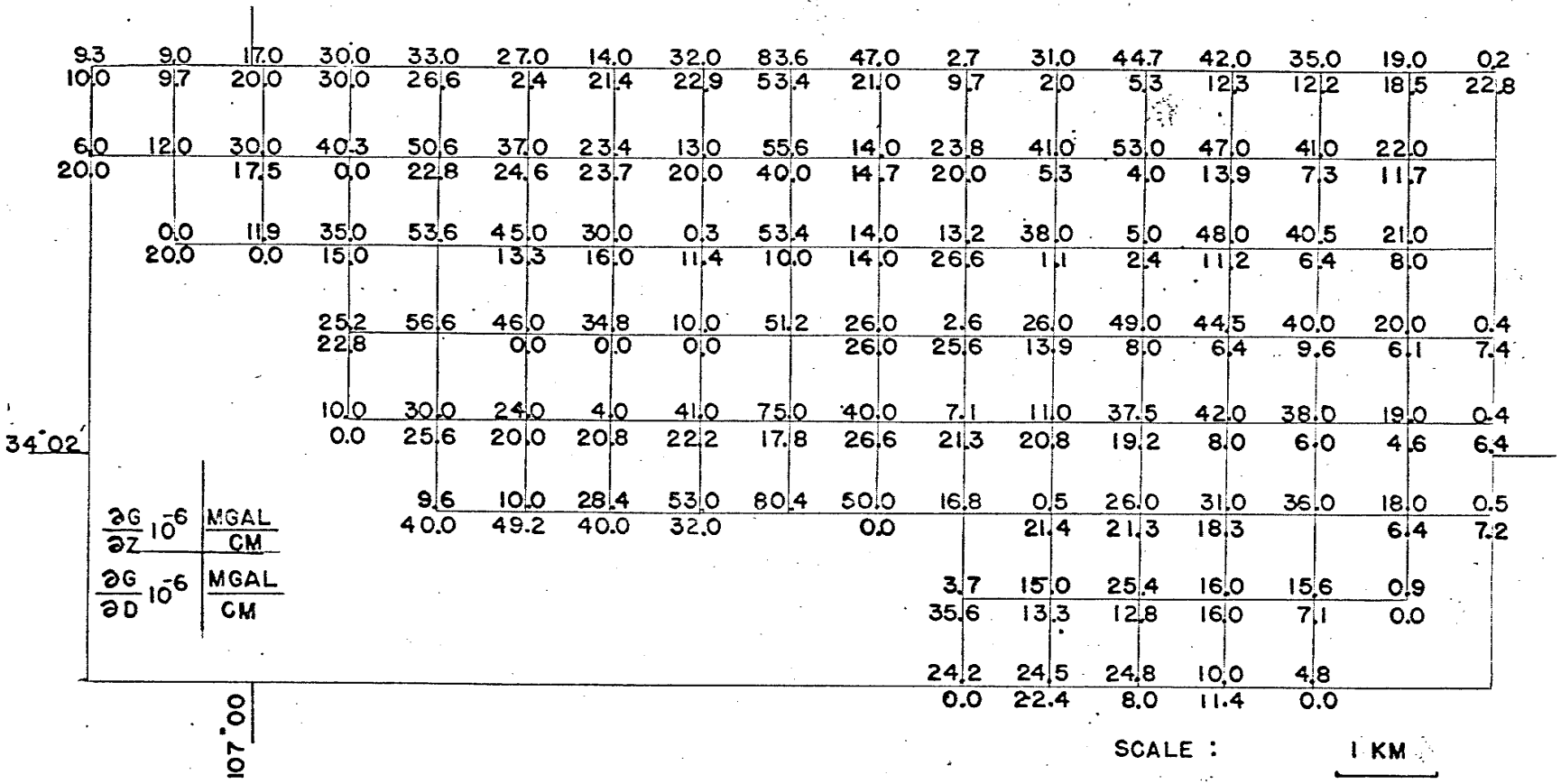

FIG. 1 VERTICAL AND HORIZONTAL GRADIENT OF THE GRAVITY

within that interval. g_d was calculated every half a mile on a square grid (see Figure 1).

Determination of the Vertical Gradient g_z . The Ackerman and Dix (1955) method was used to derive the vertical gradient of the gravity. The expression of the average of the second vertical derivative of the gravity (in cylindrical coordinates) around a circle lying in the horizontal plane passing trough the origin of the axes is

$$\frac{\partial^2 g(r,0)}{\partial z^2} = \frac{1}{2\pi}\int_0^{2\pi} \frac{\partial^2 g(r,0,\theta)}{\partial z^2}\, d\theta, \qquad (14)$$

and the expression for the vertical gradient of the gravity at the center of the circle is

$$\frac{\partial g(0,0,0)}{\partial z} = \int_0^{\infty} \frac{\partial^2 g(r,0)}{\partial z^2}\, dr. \qquad (15)$$

As an analytical expression of $\frac{\partial^2 g(r,0)}{\partial z^2}$ is not known, this integration is carried out graphically.

The second vertical derivative map of the gravity, shown in Plate V, was computed from the Bouguer anomaly map by the grid method

$$\frac{\partial^2 g(r,0,\theta)}{\partial z^2} = \frac{4}{r^2}\left[g_0(r,0,\theta) - \frac{\Sigma g_i(r,0,\theta)}{n} \right] \qquad (16)$$

where $\frac{\Sigma g_i}{n}$ is the average of discrete values of the gravity on a circle of radius r, and g_0 the value of the gravity at the center of the circle. In this work n was chosen equal to 4 and r equal to $\frac{1}{\sqrt{2}}$ mile.

In this analysis, $\frac{\partial^2 g(r,0)}{\partial z^2}$ was approximated by the averaging of discrete values of $\frac{\partial^2 g(r,0,\theta)}{\partial z^2}$ around circles of radius

$r = (300 \times a)$ m ($a = 1, 2, 3, \ldots$). Four points were used for the first circle, eight for the second and sixteen for the rest. The greater the radius of the circle, the greater is the probability of the values of $\frac{\partial^2 g(r,\theta,\theta)}{\partial z^2}$ to cancel one another, so that the function $\frac{\partial^2 g(r,0)}{\partial z^2}$ converges. $\frac{\partial^2 g(r,0)}{\partial z^2}$ was plotted versus the radius r of the circles and the curve was intergrated graphically. The values of $\frac{\partial^2 g(r,0)}{\partial z^2}$ may oscillate about zero at larger values of r, but the accuracy obtained is sufficient if the integration is carried out to the point where $\frac{\partial^2 g(r,0)}{\partial z^2}$ first reaches the value zero. $\frac{\partial g(0,0,0)}{\partial z}$ was calculated every half mile on the same grid as was g_d (see Figure 1).

Now all the terms between the brackets in equation (11) are known for each point of the grid of Figure 1. The resultant calculated anomaly $\frac{Z}{I/G\rho}$ was plotted and contoured in figure 2. This map is restricted to a small part of the magnetically surveyed area, because the Bouguer anomaly map does not extend to the south and thus restricts the calculation of the second vertical derivative map. Consequently for certain points along the southern margin, the point of convergence of $\frac{\partial^2 g(r,0)}{\partial z^2}$ was not reached and the integration of the second derivative could not be performed. The common part of the observed magnetic map and the computed magnetic map does not show any resemblance. Thus in this case, the theory of combined analysis is not applicable.

The second vertical derivative of the gravity calculated by the grid method is dependent on the radius of the circle

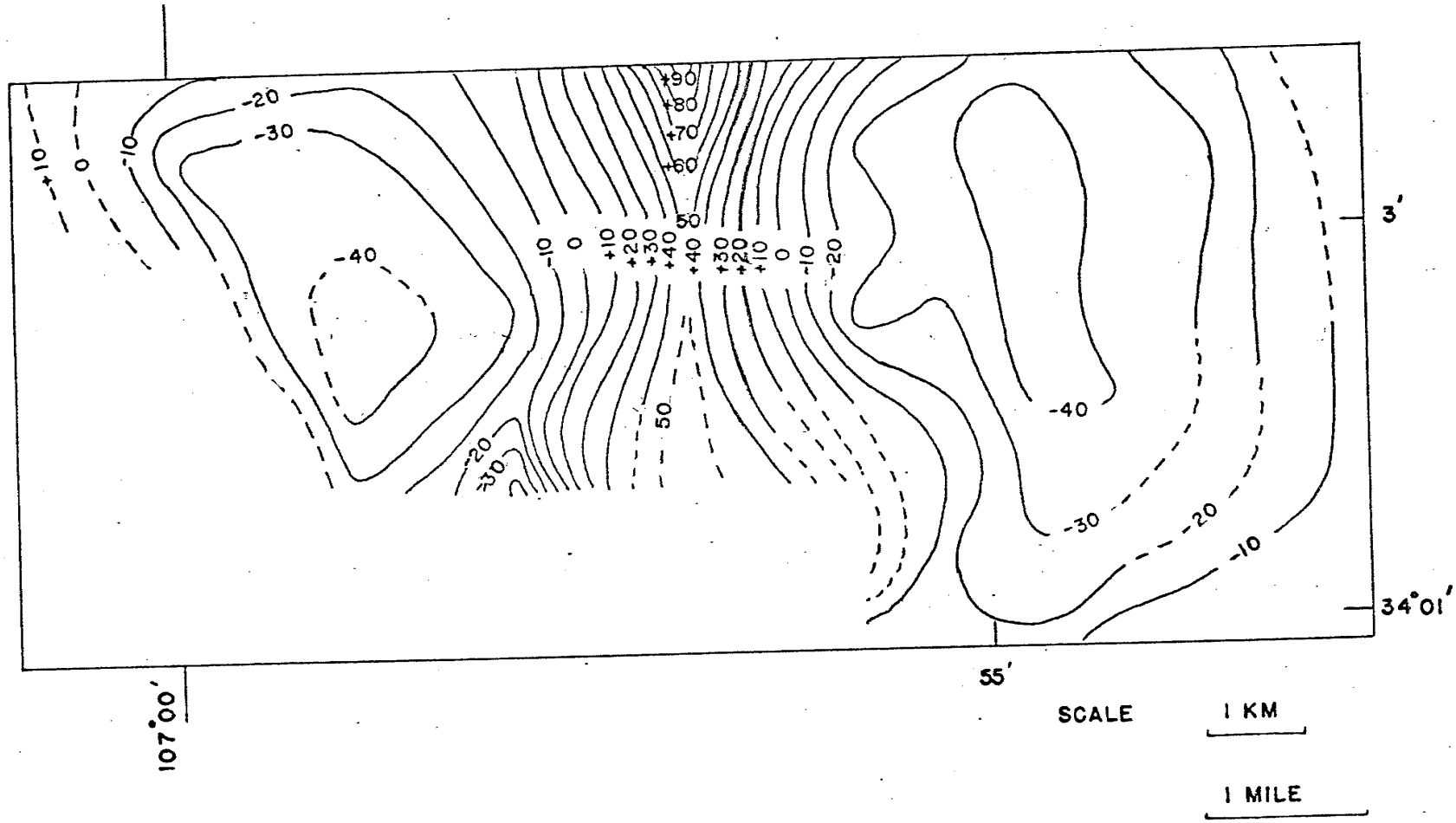

Figure 2 Computed Map of $\frac{I}{G\rho}$

used. In this work, r was arbitrary taken equal to $\frac{1}{\sqrt{2}}$ mile. One might ask whether another choice of radius could lead to a positive correlation between the observed and calculated magnetic maps.

To a certain extent, the choice of the radius does affect the shape and the magnitude of the second derivative anomalies. However the choice of r does not alter the positions of the maxima and minima. So the observed and computed magnetic maps can never match, regardless of the value of r used for the computation of the second derivative of the gravity.

The theory of combined analysis of gravity and magnetic anomalies assumes that the same structure is responsible for both anomalies. Inasmuch as the anomalies on the computed map do not match the anomalies on the observed map, we must assume that the densest rocks are not necessarily the most magnetic. The gravity anomalies may be due to prevolcanic rocks, for example Pennsylvanian limestones or Precambrian granites, that are denser than the Tertiary volcanic rocks (Anderson 1953).

Structural Interpretation of the Anomalies

Regional and Residual Magnetic Anomaly Maps

The corrected magnetic anomaly map (Plate III) represents the effects of all structures, shallow as well as deep. It is desirable to separate the contribution of shal-

low structures. The method of separation used here has been described by Griffin (1949). He defined the residual anomaly or the effects of shallow structures as

$$\Delta Z = Z_o - \overline{Z}(r) \qquad (17)$$

where

$$\overline{Z}(r) = \frac{1}{2\pi}\int_0^{2\pi} Z(r,\theta)\, d\theta , \qquad (18)$$

is the average magnetic field at the radial distance r from the point where the field is Z_o. The average value $\overline{Z}(r)$, assigned to the center of the circle, represents the effects of deep-seated structures or the regional anomaly. In this work the value of r selected was $\frac{1}{\sqrt{2}}$ mile and 4 equally spaced points were used for averaging. The resultant residual and regional maps are shown in Figure 3 and Plate VI.

The regional magnetic anomaly map (Plate VI) shows:

1) Anomaly A, a long magnetic high striking NE-SW and extending into the Rio Grande Valley to the east.

2) Anomaly B, a regular magnetic high nearly over the Black Mountain area.

3) Anomaly C, an assymetrical magnetic high on the western part of the map.

Anomaly A

Method of Interpretation. Anomaly A shows contour lines that are almost parallel, which is suggestive of a tabular struc-

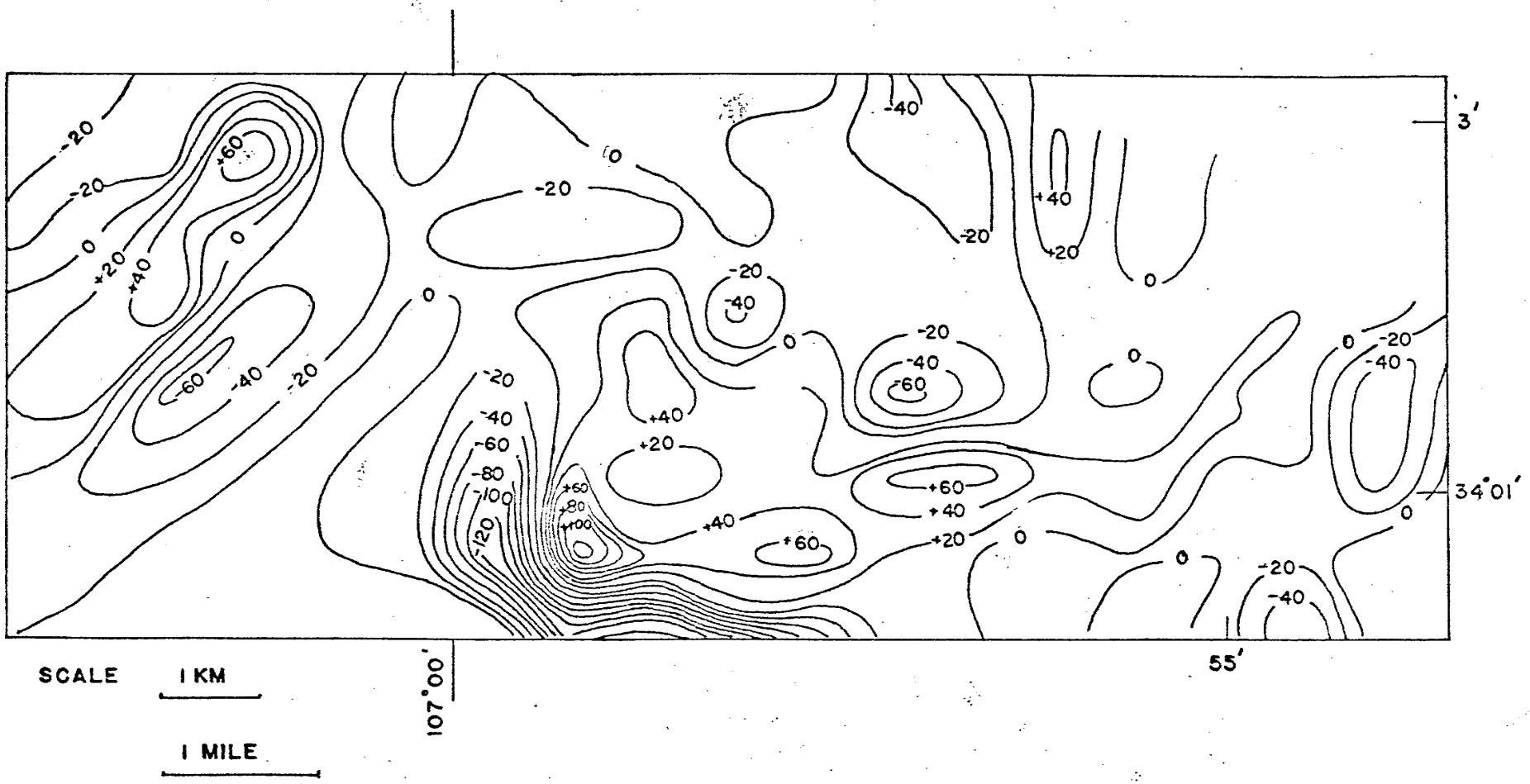

FIG. 3 RESIDUAL MAGNETIC ANOMALY MAP (IN GAMMAS)

ture. The method described by Gay (1963) was used for the interpretation of this anomaly. Gay showed that the vertical, horizontal and total intensity magnetic anomalies for long tabular bodies belong to a single mathematical family of curves for all values of dip and strike and all values of inclination of the magnetic field. In the case of a thick tabular body (see Figure 4), the expression of the anomaly at P is

$$\Delta F = C_F \left(\frac{\psi_1 - \psi_2}{R} \cos\theta_F + \frac{1}{R} \log \frac{\cos\psi_2}{\cos\psi_1} \sin\theta_F \right). \qquad (19)$$

C_F is a coefficient , R is the ratio $\frac{W}{Z}$ and θ_F is equal to $I_o' - \delta$, where δ is the dip of the plane of the body and I_o' the inclination of the component T_o' of the total field in a plane perpendicular to the plane of the body. The shape of the anomaly is defined by the function

$$f(\psi, \theta_F, R) = \frac{\psi_1 - \psi_2}{R} \cos\theta_F + \frac{1}{R} \log \frac{\cos\psi_2}{\cos\psi_1} \sin\theta_F . \qquad (20)$$

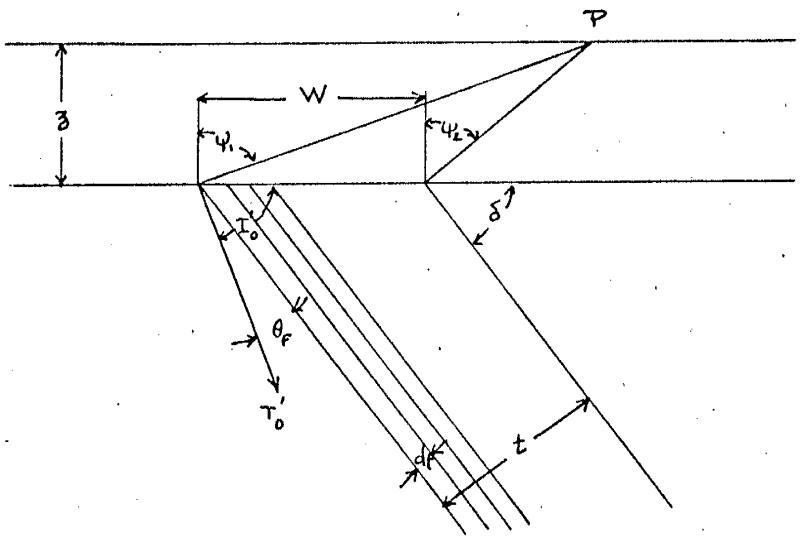

Fig. 4 Geometry of a thick tabular body

Gay has plotted values of $f(\psi, \theta_F, R)$ for different values of θ_F and R along profiles perpendicular to the body. The horizontal distance is expressed as a function of the depth z to the apex of the body. In order to facilitate the curve matching, he normalized the curves to a constant unit amplitude.

Interpretation procedure..On the magnetic map (Plate VI), the tabular structure strikes N 32°E. A profile FF' was drawn perpendicular to the strike and across the most regular part of the anomaly (see Figure 5A). Its amplitude was reduced to a unit amplitude and the profile redrafted at the scale of the standard curves. In order to match one of the standard curves, it was again reduced in the horizontal direction. Both reductions were done with a proportional divider. After many trials, the best fit was given by the standard curve having the parameters θ_f equal to -10 and R equal to 2 (see Figures 5B and 6).

The dip of the structure is

$$\delta = I_o' - \theta_F . \qquad (21)$$

If α is the strike of the structure with respect to the magnetic meridian, the inclination I_o' is given by the relation

$$\tan I_o' = \frac{\tan I_o}{\sin \alpha} , \qquad (22)$$

where I_o is the inclination of the total magnetic field. In the present case α is equal to 19° and I_o equal to 62°. I_o'

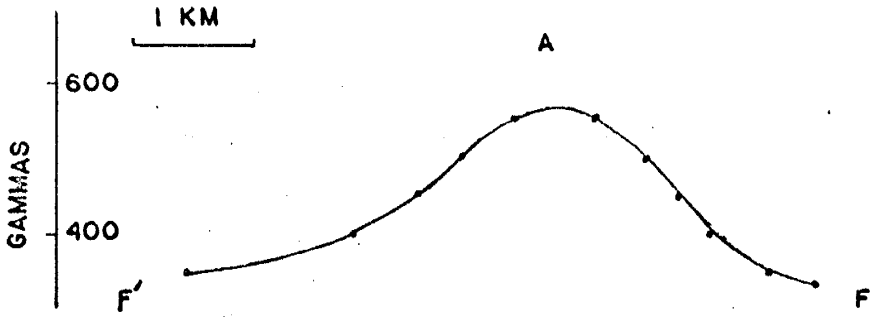

Profile at the scale of the magnetic map

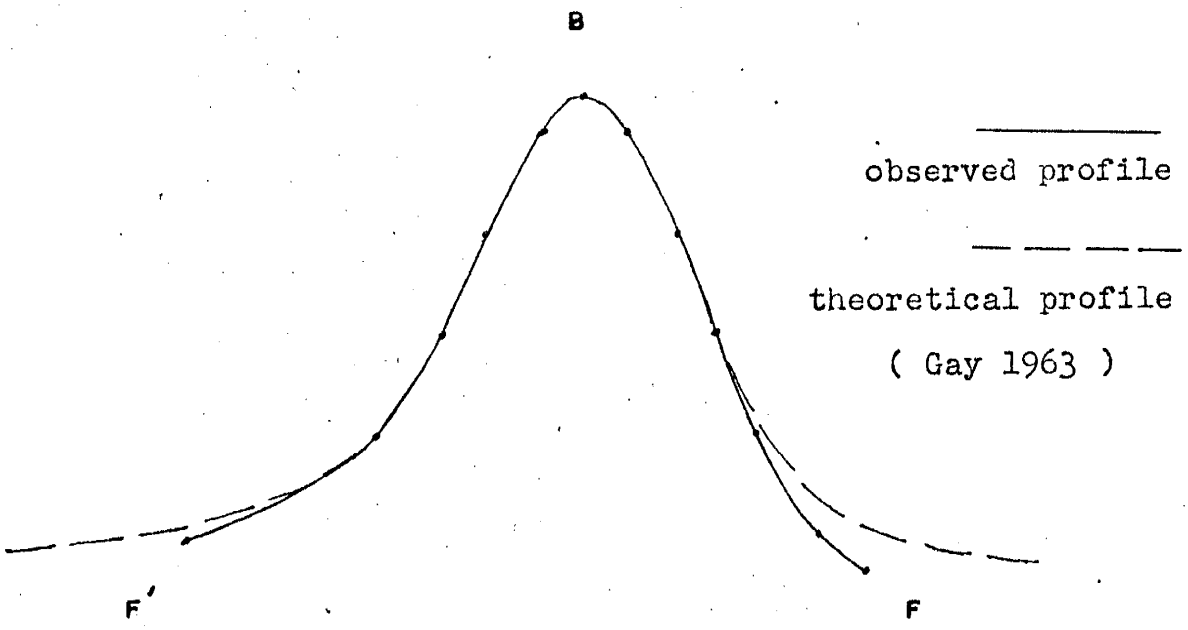

Profile at the scale of the standard curve

(Gay 1963)

Figure 5 Profile FF' (Anomaly A)

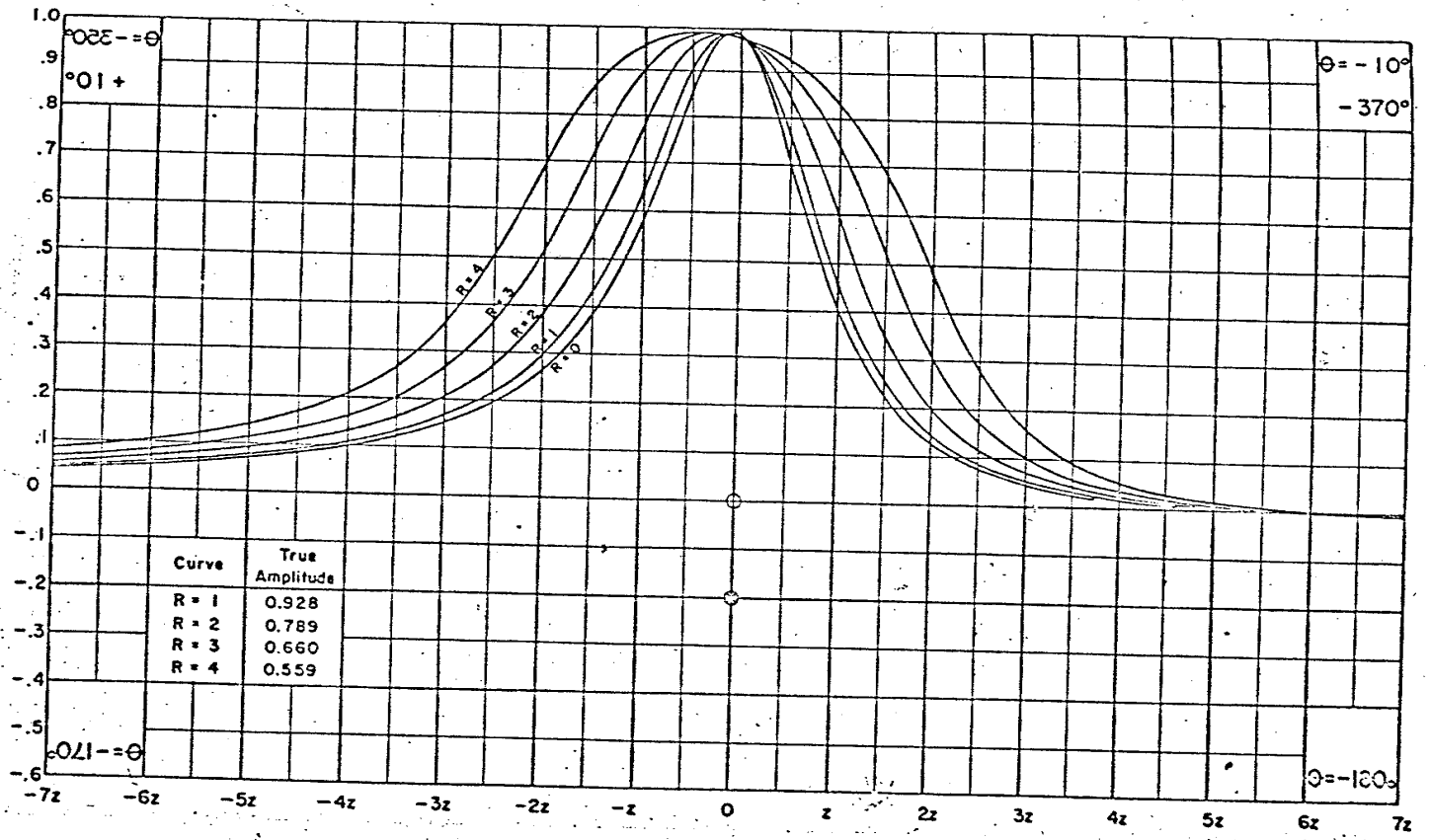

Fig. 6 Normalized curves for infinite, thick dikes

is evaluated to be 80° and equation (21) gives a value of the dip of 90°, or the tabular structure is vertical.

Since the amount of reduction applied to the horizontal scale was known, the depth of the structure could be determined by the distance on the observed profile corresponding to unity on the standard curve. The depth to the top of the structure was found to be 735 m.

The thickness of the tabular structure is given by the relation

$$R = \frac{W}{z} , \qquad (23)$$

where W is equal to t, since the structure is vertical (see Figure 4). The calculation yields a thickness of 1470 m. The thickness of the structure is also given by the equation

$$t = \frac{A z}{2k T_o' a} , \qquad (24)$$

where A is the amplitude of the observed profile and a the actual amplitude of the function $f(\varphi, -10, 2)$. The value of a for each standard curve is given by Gay (see Figure 6). The component T_o' of the total magnetic field in a plane perpendicular to the body can be calculated from the equation

$$\frac{T_o'}{T_o} = \frac{\sin I_o}{\sin I_o'} , \qquad (25)$$

where T_o is the strength of the total magnetic field. At Socorro the total magnetic intensity is 52,256 γ so T_o' is equal to 46,769 γ. All the terms in equation (24) are now

known except k, which can be solved. The susceptibility k was found to be 1626. 10^{-6} cgs. Refering to the magnetic susceptibility table (Table I), this value of k corresponds to that of the weathered basalt.

Remarks on the Interpretation of the Anomaly A. Anomaly A broadens to the north east. Two explanations can be offered for the broadening:

1) The tabular body plunges to the NE

2) The fault that limits Socorro Mountains to the east (see Plate I) may have cut through the structure and the eastern portion of the structure is now downthrown.

Anomaly B

Except for a protrusion to the east, which is due to the tabular body studied before, the shape of Anomaly B is almost circular, which suggests a spherical or cylindrical structure. The spherical structure is geologically improbable and was not considered. The model adopted was a vertical cylinder extending an infinite distance downward.

The anomaly due to an infinite vertical cylinder in a vertical inducing magnetic field is (Nettleton 1942)

$$Z = \frac{\pi R^2 z I}{(r^2 + z^2)^{3/2}}, \qquad (26)$$

where R is the radius of the cylinder, z the depth to the top of the cylinder and r a radial distance from its axis. At the point of intersection M of the plane of observation and the

axis of the cylinder, the anomaly is maximum and equal to

$$Z_M = \frac{\pi R^2 I}{z^2} . \qquad (27)$$

At a point at a radial distance $\frac{z}{2}$ from the axis of the cylinder, the anomaly is

$$Z_{r=z/2} = \frac{\pi R^2 I}{(5/4)^{3/2} z^2} . \qquad (28)$$

The ratio of $Z_{r=z/2}$ to Z_M equals 0.717. Knowing the amplitude Z_M of the anomaly, the depth to the top of the cylinder is equal to twice the radial distance at which the value of the anomaly is $0.717 \times Z_M$.

Three profiles were drawn across the anomaly B (see Plate VI and Figure 7) From these profiles the amplitude of the anomaly was estimated to be 730 γ. The radial distance at which the anomaly is equal to $0.717 \times 730 = 522\ \gamma$ was found to be 1.15 km, which gave a depth to the top of the cylinder of 2.3 km.

Assuming the anomaly caused by a structure of basaltic composition with a magnetic susceptibility of 3050. 10^{-6} cgs (the highest value given by the bridge for the basalt), the intensity of magnetization in the vertical cylinder due to a vertical inducing magnetic field of 46,050 γ is $I = kZ = 142\ \gamma$. If ω is the solid angle subtended by the top of the cylinder viewed from a point on the plane of observation, the value of the anomaly at that point is

$$Z = I\omega \qquad \text{(Nettleton 1942)} \qquad (29)$$

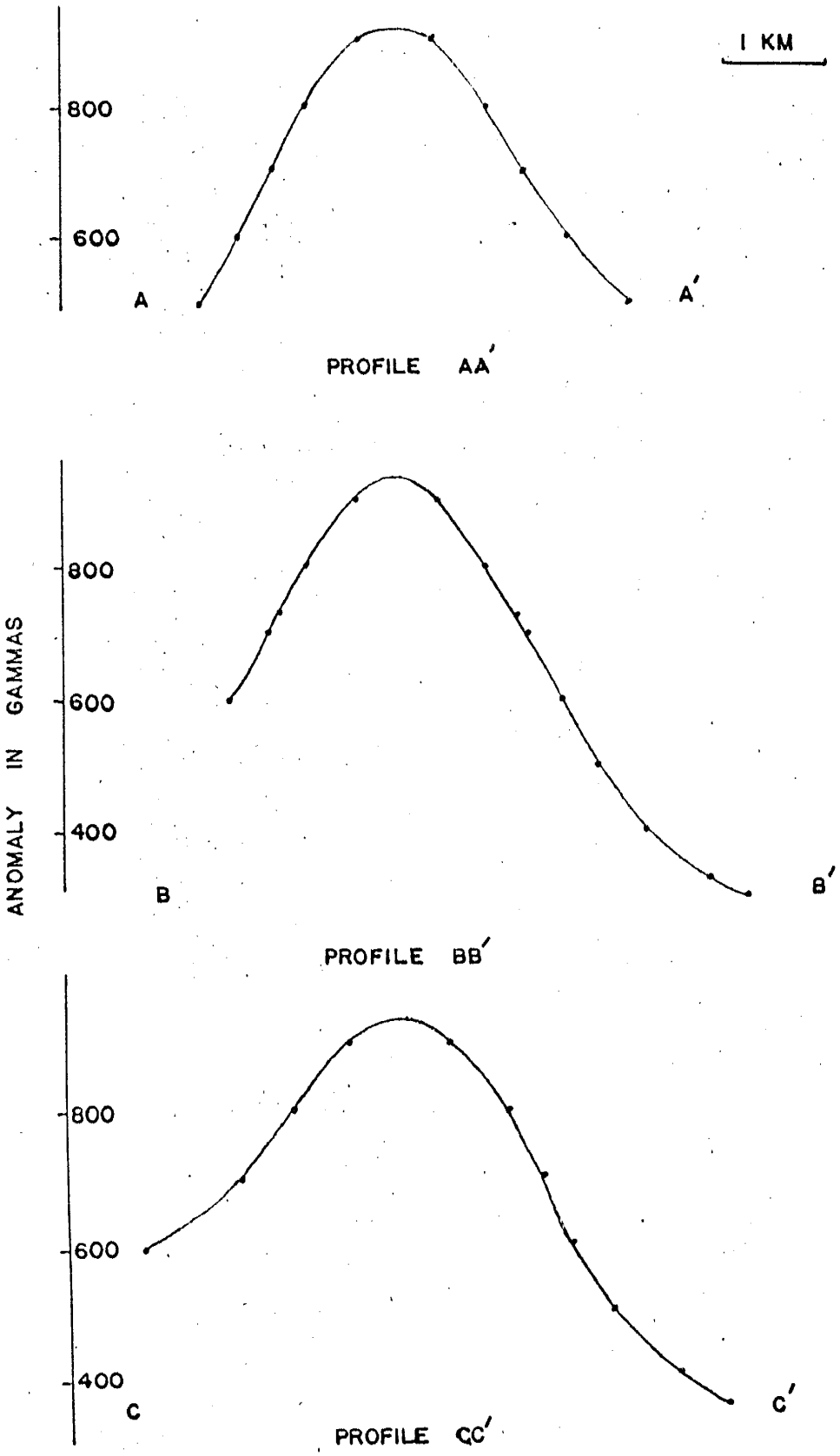

Figure 7 Anomaly B

In order to get the maximum value of the anomaly (730γ), the solid angle at the point M on the axis of the cylinder would have to be $\omega = \frac{730}{142} = 5.15$. This value is close to 2π which means the cylinder would have to be extremely broad. The anomaly for such a broad structure could not match the observed profile. As an alternative, a value of 24000. 10^{-6} cgs was adopted for the susceptibility of the cylinder (see Section on Magnetic Susceptibility Measurements). Neglecting the susceptibilities of the surrounding rocks, the intensity of magnetization of the structure is 1105γ. Equation (27) can be written in the form

$$R^2 = \frac{Z_M \delta^2}{\pi I} . \qquad (30)$$

The radius of the cylinder calculated with equation (30) is 1.05 km. Using the chart of solid angles shown in Figure 8 (Nettleton 1942), the anomaly over the cylinder was computed. The resultant profile matched the observed profile (see Figure 9).

It is interesting to note here that the residual magnetic map (Figure 3) shows on the south western edge of Anomaly B a sharp anomaly limited in size. This may be due to a projecting apophyse from the stock or a volcanic neck.

Anomaly C

The high anomaly striking NE-SW on the western part of the magnetic map (Plate VI) may be due to a flow of highly magnetic rock, that has been buried under sediments. Such a

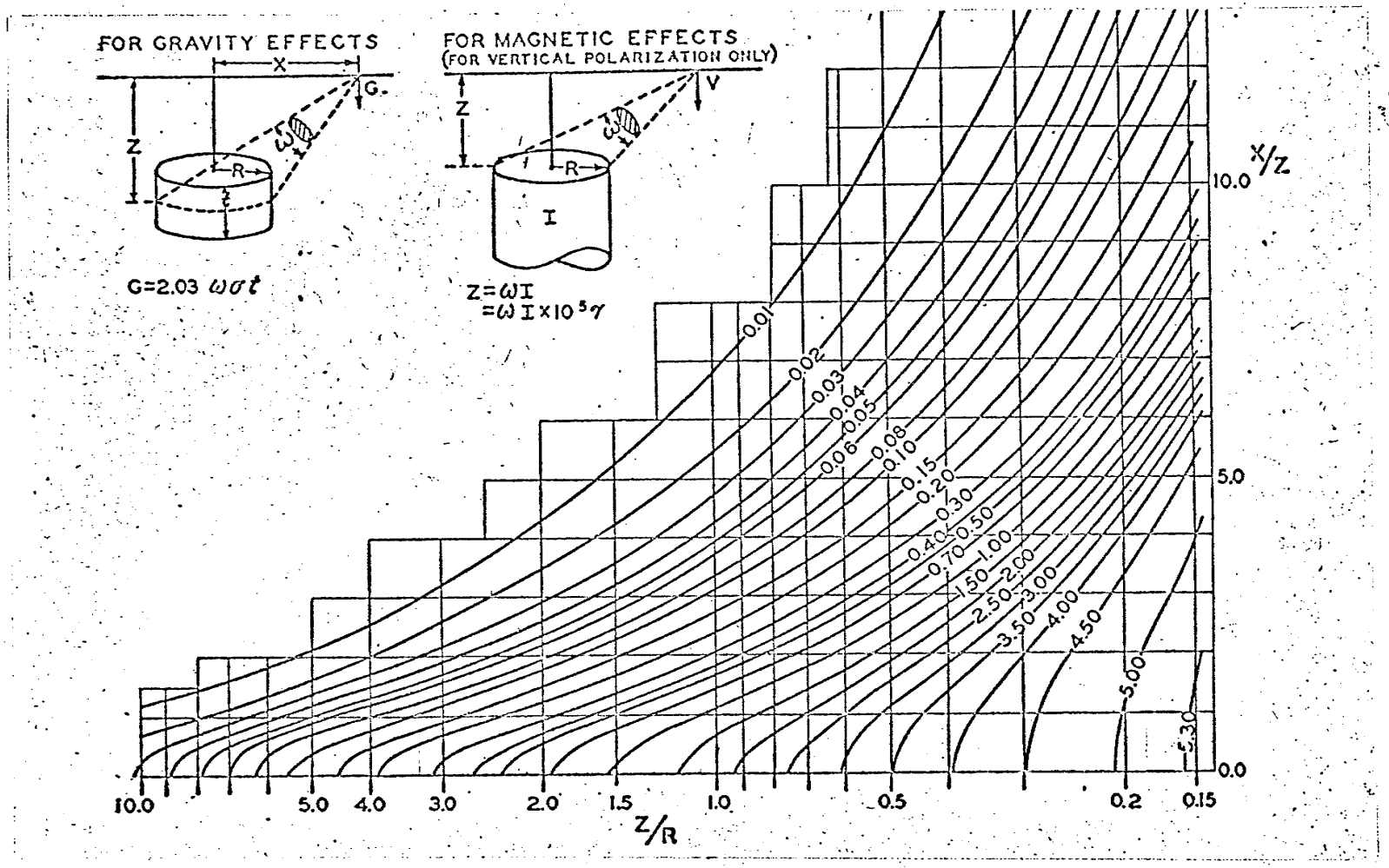

Fig. 8 Solid angle for horizontal circular discs

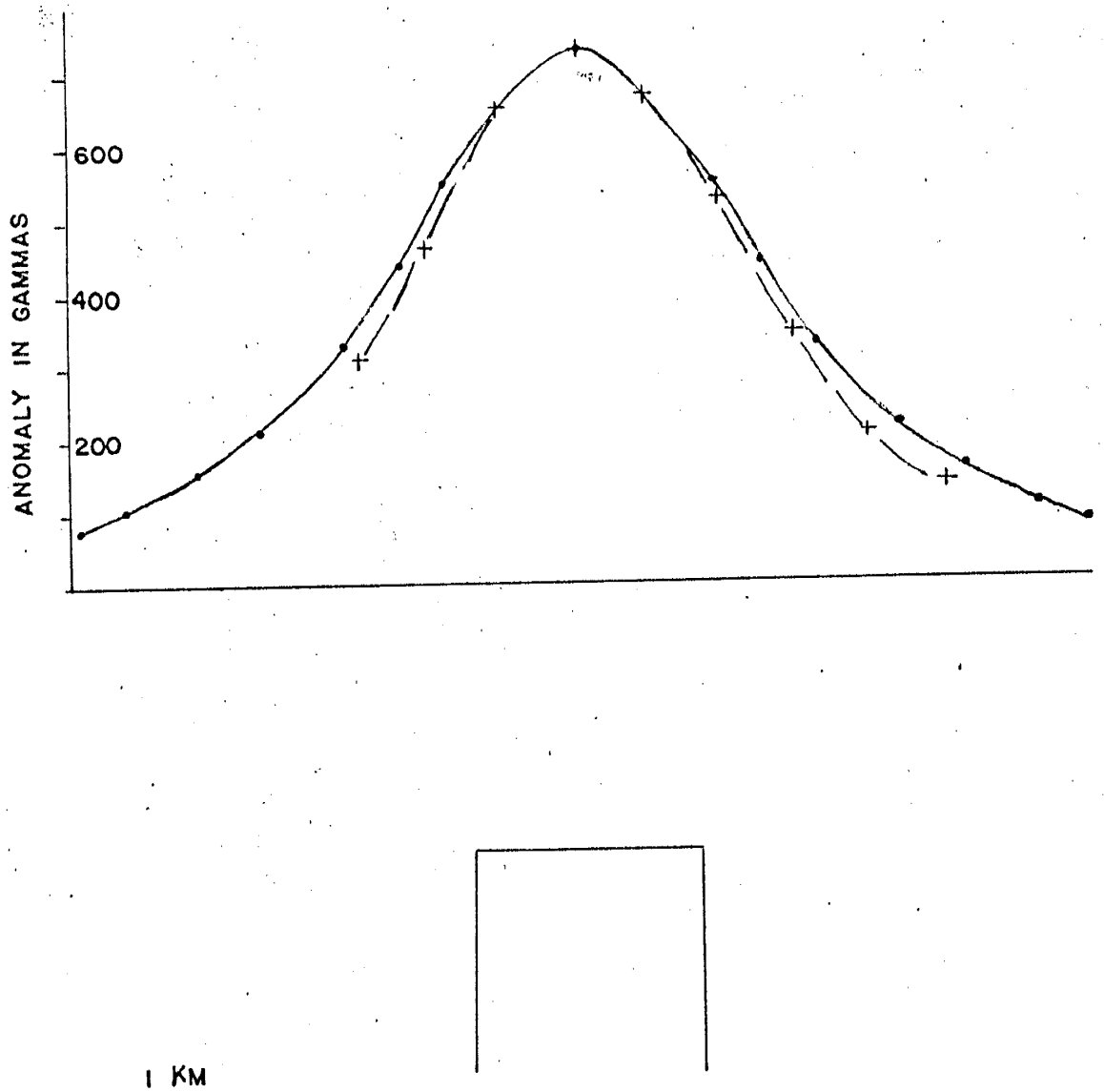

——————— computed profile

——— — ——— observed profile

(average of the profiles AA', BB', CC')

Figure 9 Anomaly B

structure is observable in the area south of US Highway 60 (M. Willard, personal communication). No computation was attempted here, because there is no geological control that allows any judicious assumptions as far as the position, thickness, and susceptibility of the flow are concerned.

CONCLUSION

The magnetic survey of the southern part of Socorro Mountains shows simple and broad anomalies. On the basis of the surface geology of the area, intrusions of basic rocks or flows of basic rocks were assumed responsible for the high anomalies. Although Anomaly B and Anomaly C cover areas where flows of basalt can be observed, there is no correlation between the visible geological structures and the anomalies. In fact the broadness and low gradient of the anomalies suggest deep-seated structures.

On the basis of the shape and magnitude of the anomalies and the susceptibilities of the rocks collected from the area surveyed as well as from the region south of US Highway 60, two structures were computed.

Anomaly A was interpreted as due to a long vertical tabular body, 1470 m wide and buried at a depth of 735 m. The susceptibility of the rock it is composed of (1626. 10^{-6} cgs) corresponds to the average value of the susceptibility of the basalt of the area.

Anomaly B was interpreted as due to a stock of basaltic composition having a susceptibility of 24,000. 10^{-6} cgs. The diameter of the stock is 2.1 km and the depth to the top is 2.3 km. This stock may be the source of the basalt flow that constitutes the upper portion of Black Mountain and the surrounding basalt outcrops.

REFERENCES

Ackerman H.A. and Dix C. H.,"The First Vertical Derivative of Gravity ", Geophysics, vol. 20 (1955)

Anderson R. C., " A Gravity Survey, Rio Grande Valley, Socorro, N.M. ", Master of Science thesis. NMIMT (1953)

Dobrin M. B., Introduction to Geophysical Prospecting, McGraw-Hill Book Company, Inc. (1960)

Garland G. D., " Combined Analysis of Gravity and Magnetic Anomalies ", Geophysics, vol. 16 (1951)

Gay S. P. Jr., " Standard Curves for Interpretation of Magnetic Anomalies over long Tabular Bodies ", Geophysics, vol 28 (1963)

Griffin W. R., " Residual Gravity in Theory and Practice " Geophysics, vol. 14 (1949)

Johnson D., " A Magnetometric Survey of the Iron Horse Magnetite Deposit, Socorro County, New Mexico " Master of Science thesis (NMIMT) (1953)

Lundbak A., " Combined Analysis of Gravimetric and Magnetic Anomalies and some Paleomagnetic Results ", Geophysical Prospecting, vol 4 (1956)

Nettleton L. L., " Gravity and Magnetic Calculations ", Geophysics, vol. 7 (1942)

Stephens R. R., " The vertical Magnetometer ", Report for the course Geophysics 452 (NMIMT) (1962)

This thesis is accepted on behalf of the faculty of the Institute by the following committee:

Allan R. Sanford

Max Edelbaum

Clay T. Smith

Charles R. Holmes

Date: August 10, 1965

Qal Sediments of arroyos. Rio Grande flood plain and Snake Ranch flats

TQsf Santa Fe formation of silt, sand and gravel

TQb Basalt flows overlying Santa Fe and Popotosa formations

TQr Glassy rhyolite flows and tuff beds

Tp Popotosa formation. Red and green clays Locally interbedded basalt flows

Td Datil group: rhyolite, latite and andesite flows tuff and breccia

Symbols used in the geologic map (Plate I)

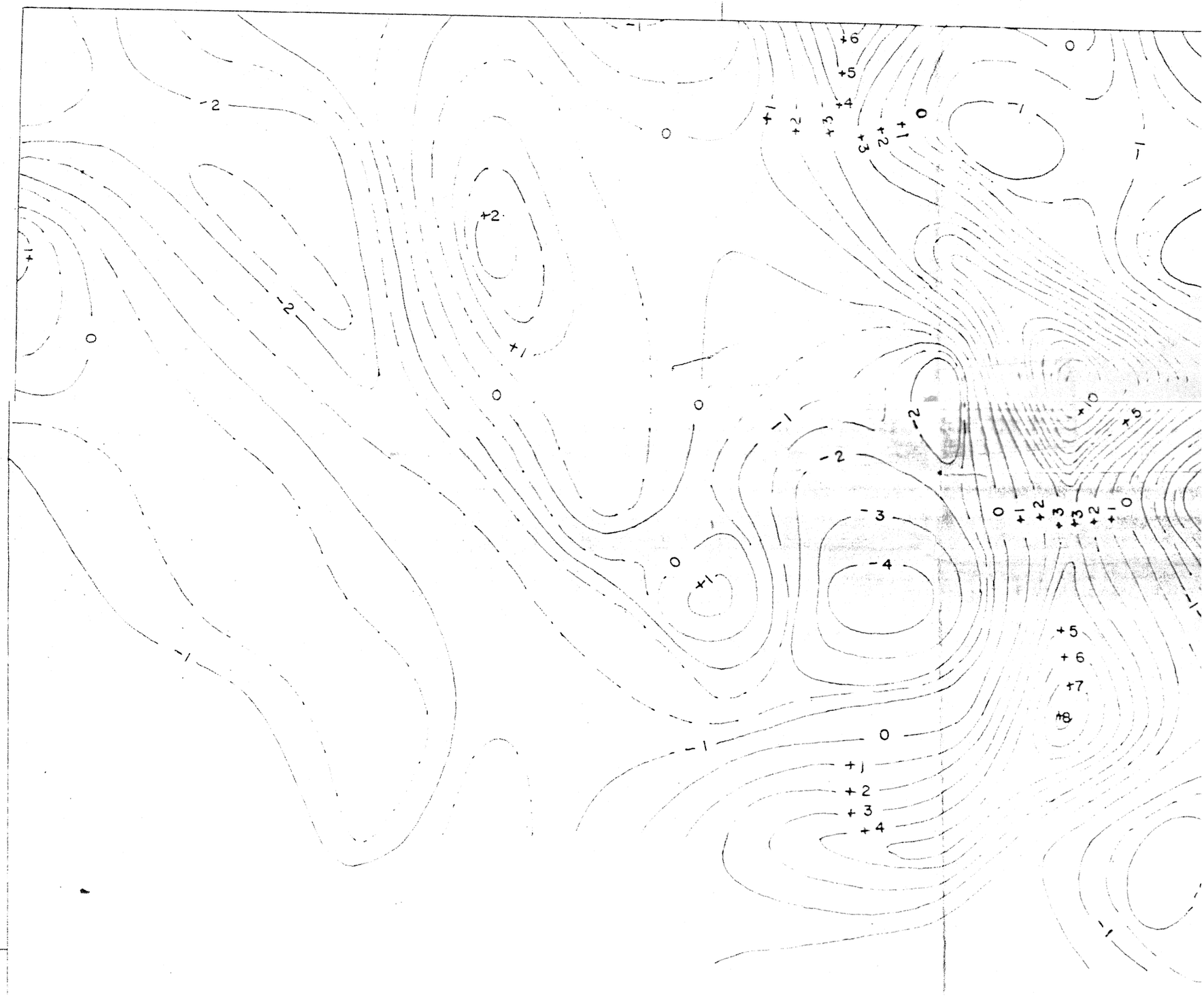

SECOND VERTICAL DERIVATIVE MAP

PLATE V

DERIVATIVE MAP (GRAVITY)

PLATE I

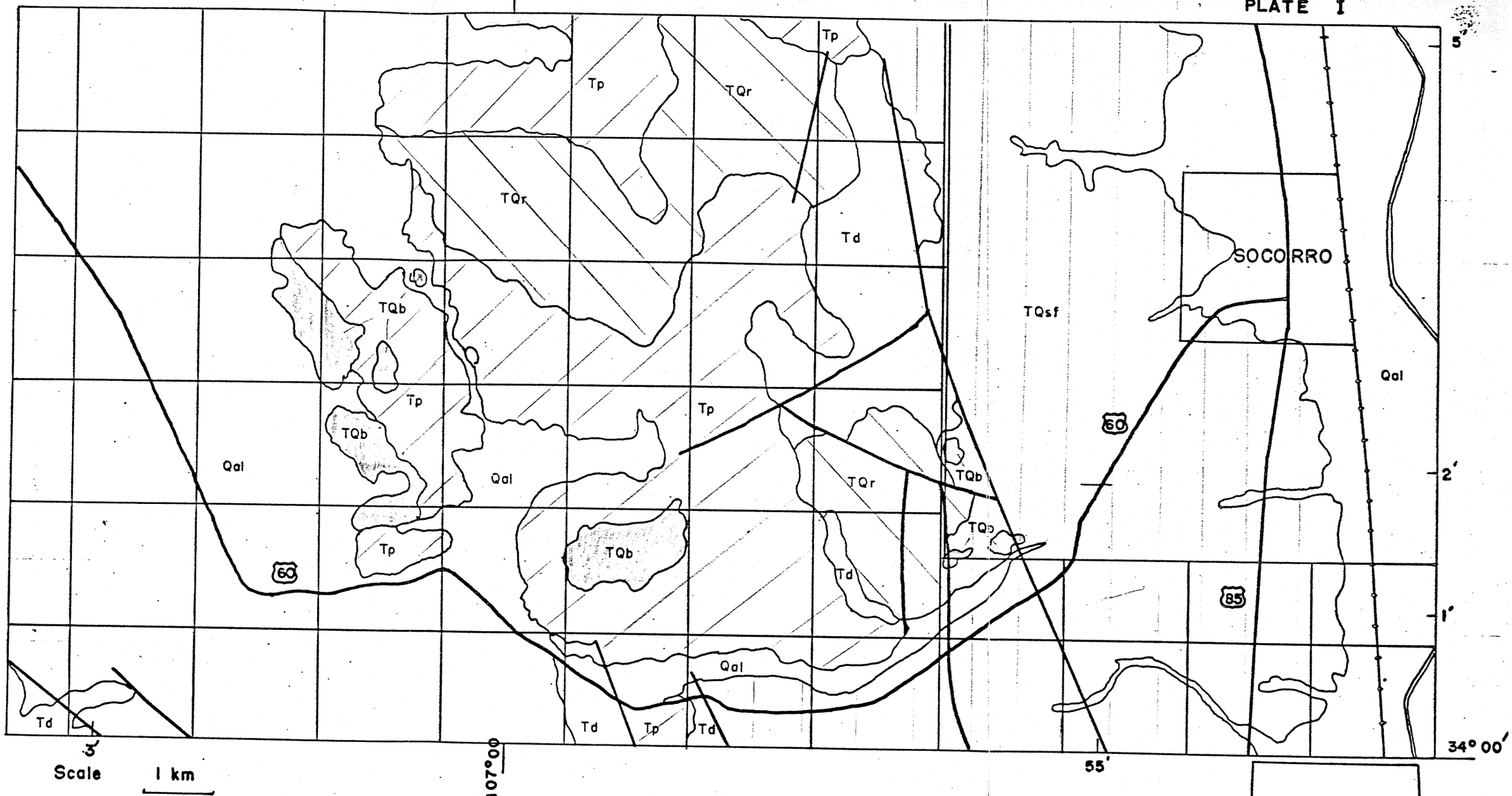

GEOLOGIC MAP OF SOUTHERN SOCORRO MOUNTAINS

by Schilling (1956)

PLATE VI

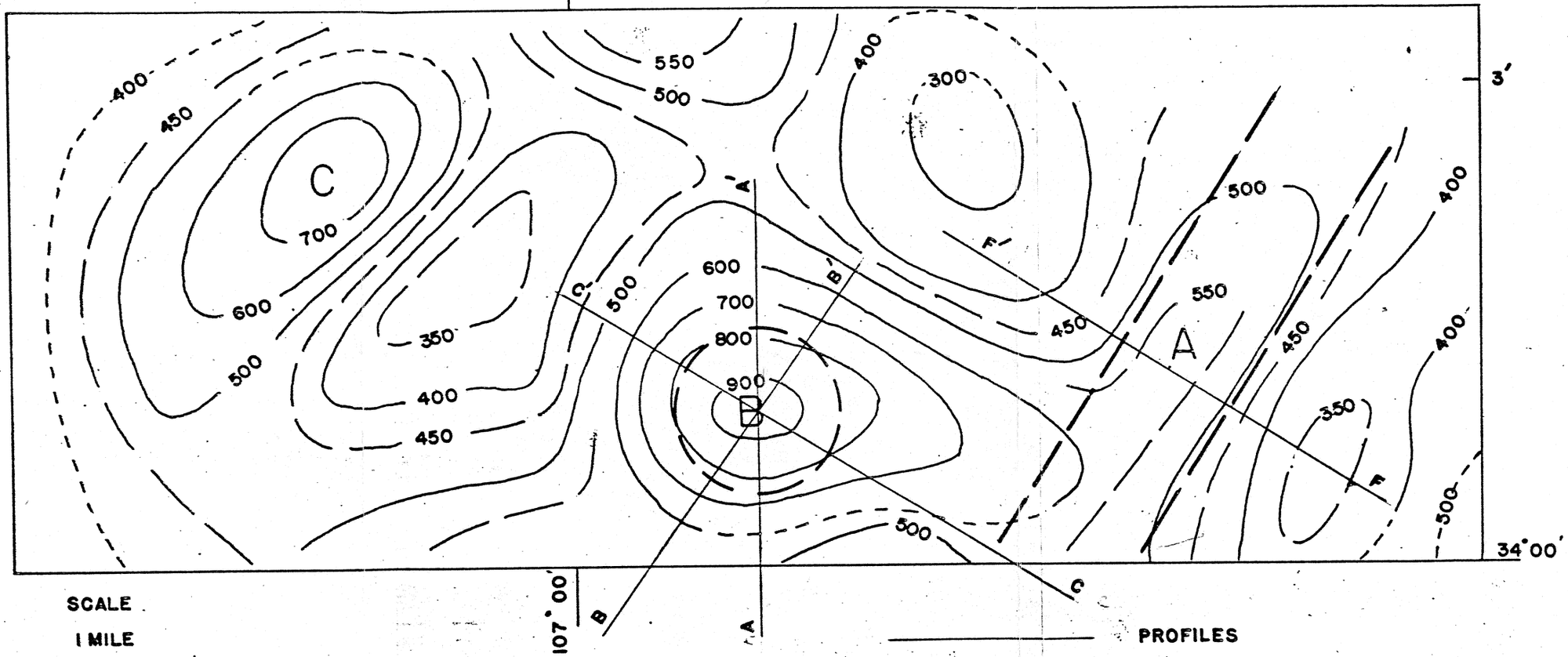

REGIONAL MAGNETIC ANOMALY MAP (IN GAMMAS)

PLATE II

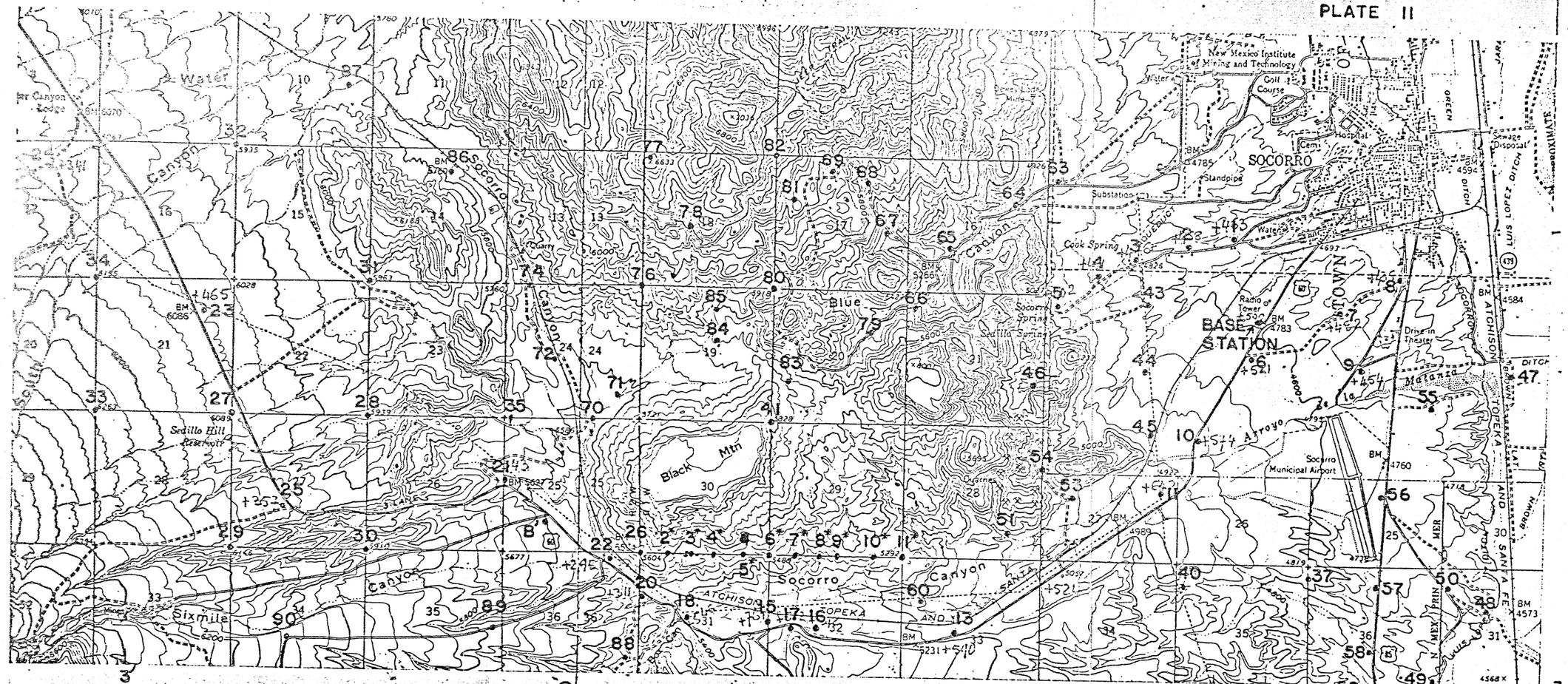
SOCORRO
BASE STATION
Socorro
Canyon
Blue
Black Mtn
Sedillo Hill Reservoir
Sixmile
Canyon
Socorro Municipal Airport
New Mexico Institute of Mining and Technology
Golf Course
Hospital
Cem.
Standpipe
Substation
Cook Spring
Sedillo Spring
Socorro Spring
Radio or Tower
Drive-in Theater
Sewage Disposal
Melonic
Arroyo
ATCHISON TOPEKA AND SANTA FE
N. MEX. PRIN. MER.
107°00'
34°00'
3
55'
SCALE 1:62 500
1 KM
1 MILE
LOCATION OF THE STATIONS

PLATE IV

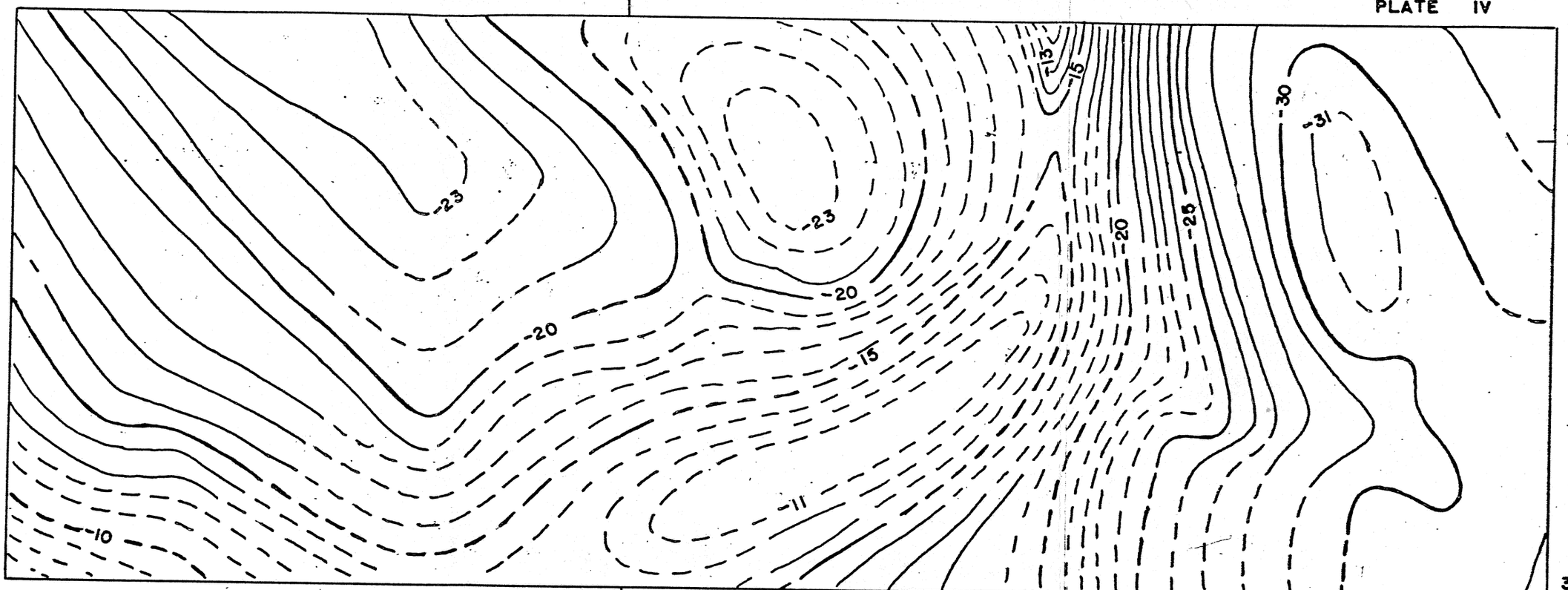

SCALE

1 MILE

1 KM

BOUGUER GRAVITY ANOMALY MAP (IN MGAL)

(FROM WORK BY A.R. SANFORD)

PLATE III

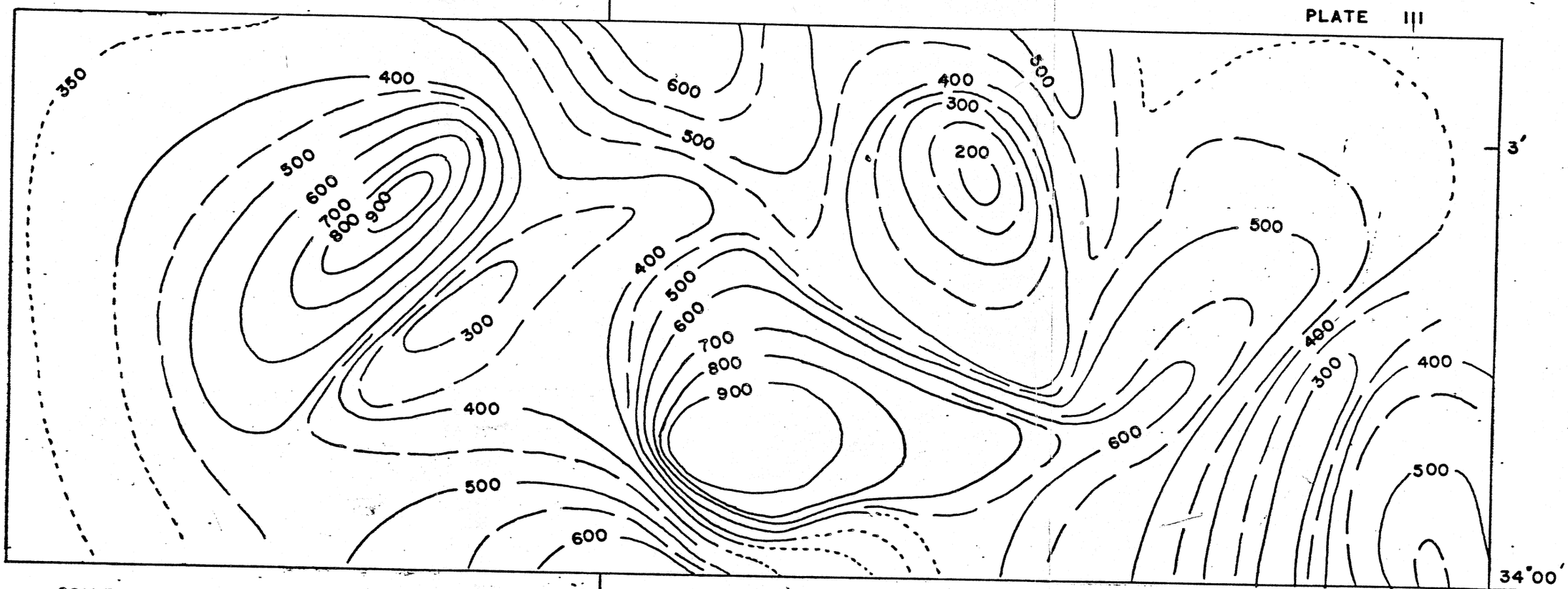

FIG. OBSERVED MAGNETIC ANOMALY MAP.

Z VERTICAL ANOMALY IN GAMMAS